ARID ZONE JOURNAL OF ENGINEERING, TECHNOLOGY & ENVIRONMENT
AZOJETE December 2024. Vol.20(4):913-925
Published by the Faculty of Engineering, University of Maiduguri, Maiduguri, Nigeria.
Print ISSN: 1596-2490, Electronic ISSN: 2545-5818
www.azojete.com.ng

ORIGINAL RESEARCH ARTICLE

OPTIMIZATION OF ARC WELDING PARAMETRIC INFLUENCE ON MECHANICAL PROPERTIES OF DISSIMILAR METALS

B. J. Olorunfemi[1], B. S. Adeleye[1], K. A. Bello[1] and O. T. Oginni[2]

[1]Department of Mechanical Engineering, Federal University Oye-Ekiti, Nigeria.
[2]Department of Mechanical Engineering, Bamidele Olumilua University of Education, Science and Technology, Ikere-Ekiti, Ekiti State, Nigeria.

**Corresponding author's email address: oginni.olarewaju@bouesti.edu.ng*

ARTICLE INFORMATION

Submitted: 04 May, 2023
Revised: 12 June, 2024
Accepted: 20 June, 2024

Keywords:
Feed rate
Hardness
Optimal process
Tensile strength
Welding parameter

ABSTRACT

Welding dissimilar metals require technical expertise to achieve moderate cost, quantity, and quality, but selecting the right parameters is challenging due to various operating conditions. The paper optimized welding process parameters for two dissimilar metals, INCONEL 625 and GL E360, focusing on mechanical properties like tensile strength and hardness. The welding process parameters were optimized using Gas Metal Arc Welding power sources, Flux Cored Wire Electrode (FCWE), design experts, and response surface methodology, and tensile strength and hardness tests were conducted. At the anticipated optimal process welding parameters of 52.86 m/s welding speed, 5.28 m/min welding feed rate, and 23.16 volts, three confirmation experiments were carried out. The study revealed that the tensile strength and hardness of the welding process significantly influenced response variables, ranging from 380 MPa to 500 MPa. The most noticeable effect was observed at a welding speed of 52 m/s, a feed rate of 5.6 m/min, and a voltage of 26 V. The empirical model's tensile strength and hardness were validated using experimental results, and the software predicted 53 welding speed, 5 welding feed rate and 23 voltages. The welding process parameters significantly impacted tensile strength and hardness, while the welding feed rate parameter had the least impact on both.

© 2024 Faculty of Engineering, University of Maiduguri, Nigeria. All rights reserved.

1.0 Introduction

Joining different materials is acknowledged as a challenge for the development of new structural components within the production industry (Stoll and Benner, 2021). The criterion for welding dissimilar components requires suitable joining expertise (Zhang-Yang *et al*., 2020). Fusion welding is a commonly used method for joining dissimilar steels (Zhang *et al*., 2020; Cooke *et al*., 2019). Optimizing weld parameters for such fusion weld joints will help in achieving a sound weld joint free of weld defects and improve productivity (Li *et al*., 2021).Metal joining is the process of joining two metal parts either temporarily or permanently with or without the application of heat and pressure by welding, soldering, brazing, riveting, adhesive bonding, assembling with bolts, and seaming (Dark *et al.,* 2021). Welding is the process of joining similar and dissimilar metals or other materials by applying heat, pressure, and filler materials. In the fusion welding process, coalescence is done by melting two parts to be joined and applying filler metals to the welded joints to provide strength. The fusion welding process is classified as the arc welding process, the resistance welding process, the radiant welding process, and the thermoelectric welding process. Manufacturers are focused on joining dissimilar materials to reduce manufacturing costs and build lightweight components. Steel structures are lighter and more cost-effective when their structural components are made of different steels (Luo *et al*., 2022). Chemical, petrochemical, nuclear, power generation, and other industries use a variety of dissimilar steel joints (Johnson and Murugen, 2020; Kumar *et al*., 2023). Joining dissimilar steels is typically more difficult than joining similar steels (Beygi *et al*., 2023; Sivasubramani *et al.,* 2021). This is caused by changes in chemical composition and thermal expansion coefficients. Tungsten inert gas welding (TIG) (Raju and Kumar, 2022), is an arc welding

process that provides outstanding welding with a coalescence of heat generated through an electric arc between a tungsten electrode and the steel (Assefa *et al*., 2022). There are five basic welding joint types commonly used in the industry, including butt joint, tee joint, corner joint, lap joint, and edge joint welding, as shown in Figure 1 (Buffa *et al*., 2022). Lap joints are commonly used for sheet metal, as depicted in Figures 1 and 2.

Gas Metal Arc Welding (GMAW) is a semi-automatic or automatic arc **w**elding process in which a continuous and consumable wire electrode and a shielding gas are fed through a welding gun (Khrais *et al*., 2023). It is developed for welding aluminium and other non-ferrous materials (Devanathan *et al*., 2022). The various welding processes are shown in Figure 3. Welding is commonly used in the areas of pipe welding and joints, automotive production and maintenance, manufacturing, shipbuilding, construction, railroad tracks, and underwater welding, both for ferrous and non-ferrous metals (Bossle *et al*., 2023). Friction stir lap welding (FSLW) involves the joining of alloys in a solid-state manner, which can mitigate the challenges due to melting and solidification (Bossle *et al*., 2023; Satputaley *et al*., 2021; Patel *et al*., 2020; Mou *et al*., 2021; Tesfaye, 2023; Kannan *et al*., 2019; Ramaden and Boghdadi, 2020). The process of GMAW requires a welding gun, a source of electric power supply, an electrode wire feed unit, and a source of shielding gas (Alagarsamy and Kumar, 2019). The advantages of gas metal arc welding include no flux. Applications of gas metal arc welding are found in semi-automated or automated industrial applications, commercially available metals, deep groove welding of plates and castings, and welding light gauge metals.

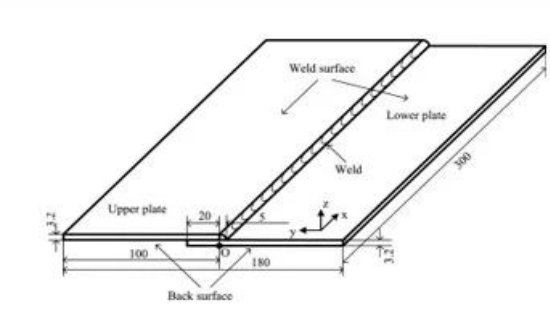

Figure 1: Lap welding joints

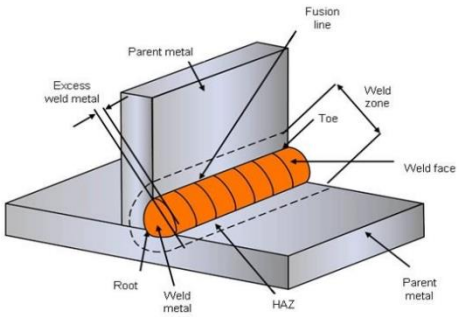

Figure 2: Fillet weld

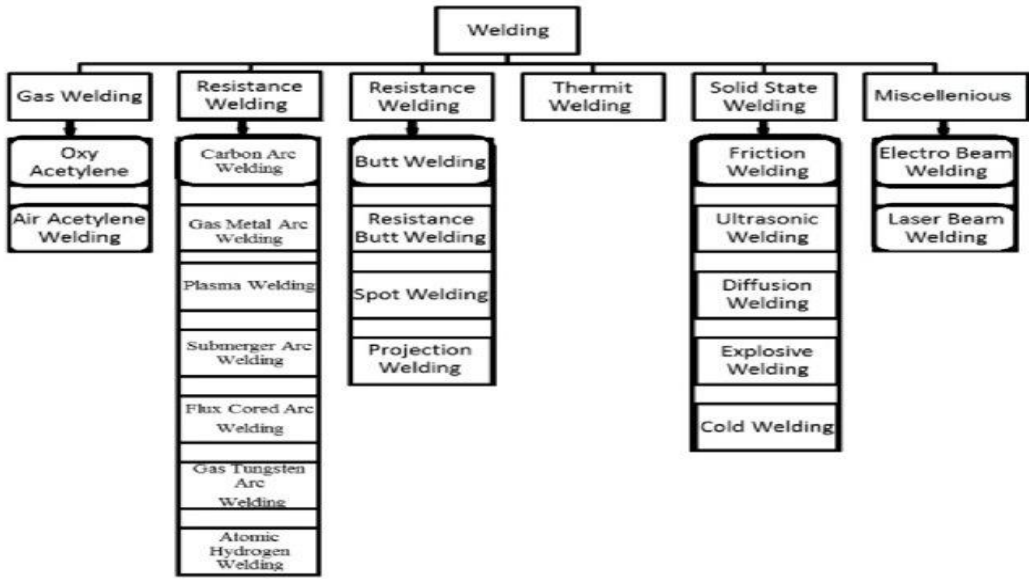

Figure 3: Various types of welding process (Buffa *et al*., 2022)

The importance of welding dissimilar metals for operation cost reduction, quality, and productivity in the welding process parameters had been studied, but it did not find out the effect of these parameters on the mechanical properties of dissimilar metal wed joints. It is necessary to determine the right GMAW parameters and processes for dissimilar metals involving high-strength steel (Inconel 625 plate) and nickel-based alloys (GL E36 steel) and their influence on the mechanical properties to eliminate the risk associated with failure and reliability of materials during their service life. Hence, the joining of these dissimilar steels finds a lot of

Corresponding author's email address: oginni.olarewaju@bouesti.edu.ng

applications in fabrication industries (Madhavadas *et al*., 2022; Arunkumar *et al*., 2022; Ren *et al*., 2022). The present study uses an optimization application approach technique to investigate the influence of welding parameters on tensile strength and hardness, enhancing the quality of the weld joints of dissimilar metals, comprising Inconel 625 and GI E36 steels, as a driver to guide the stakeholders in the manufacturing industry.

2. Materials and Methods

The materials used for carrying out the study and their specifications are: 3 mm thick Inconel 625 plate, 3 mm thick GL E36 steel plate, 5mm electrode, and a gas metal arc welding machine. The choice of the materials was made due to variations in the condition of service and specifications of the materials available, such as the size of the samples, weight, cost, availability, durability, and strength of the materials. It has good toughness properties, higher strength, strong corrosion resistance, processing properties, and welding properties.

2.1 *Experimental setup*

The GMAW power voltage 230 V single-phase flux wire welding machine was used for making buttweld joints. The mechanized torch movement ensured precise control over the weld speed, while voltage and wire feed rate were set at the GMAW power source to one decimal place precision. Flux-cored wire electrodes of diameter 3 mm suitable for this dissimilar welding were used as filler material. The 3 mm Inconel 625 plate was welded to 3mm GL E36 steel using GMAW.

Table 1 presents the chemical composition of the Inconel 625 and GL E36 steel plates. Figure 4 shows the two- and three-dimensional sectional views and lap joint configuration with plate dimensions overlapped for FSLW. The horizontal dashed and vertical dotted lines in the two-dimensional sectional view are the locations for the hardness measurement. Figures 5 and 6 are the sample microstructures.

The welded specimens were transversely cut using a diamond-plated blade, ground, and polished for microstructure evaluation. The hardness distributions were measured with a load of 500 g and at a regular gap of 0.3 mm along the dashed lines in the Y-direction. The hardness measurements were determined along the dotted line in the Z-direction at a regular gap of 0.15 mm. Figures 7 and 8 show the longitudinal and transverse welded specimens for evaluation of the joint tensile strength. Six lap-shear specimens were tested for each process condition, with the steel plate being pulled for three cases and the Inconel 625 plate being pulled for the other three samples. Separate engagement of the steel and Inconel 625 plates during the lap-shear tensile testing was conducted to evaluate the effect of stir zone asymmetry on the final weld joint strength. Figure 9 shows the longitudinal micro-tensile testing specimen and its dimensions. The Response Surface Methodology experimental design was used to vary the selection of three different process input parameters, such as welding speed, wire feed rate, and voltage, and three levels, as shown in Table 2.

Table1: Chemical composition (%) of Inconel 625 and GL E36 steel

Elements	Ni	Cr	Fe	Mo	Nb	Co	Mn	Al	Ti	Si	C
INCONEL625	58	21.70	4.70	8.60	3.38	0.03	0.09	0.13	0.18	0.18	0.02
GL E36	-	0.06	-	0.01	0.03	-	1.40	0.03	0.01	0.39	0.17

Table 2: Process Parameters and levels

Process Parameters	Level 1	Level 2	Level 3
Welding speed (s)	52.0	58.0	64.0
Wire Feed rate (F)	4.7	5.1	5.6
Voltage (volts)	22.0	24.0	26.0

Corresponding author's email address: oginni.olarewaju@bouesti.edu.ng

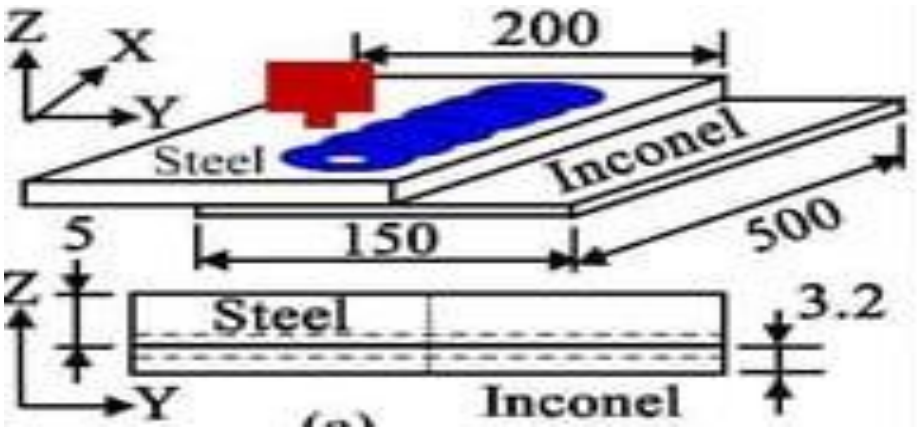

Figure 4: 2-3 Dimension Sectional View

Fig. 5: Horizontal micro structure

Fig. 6: Vertical Micro structure

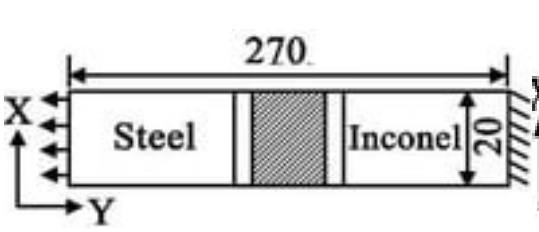

Fig. 7: Longitudinal Specimen

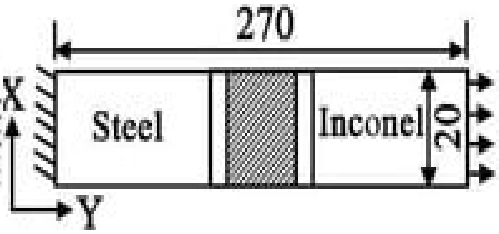

Fig. 8: Transverse Specimen

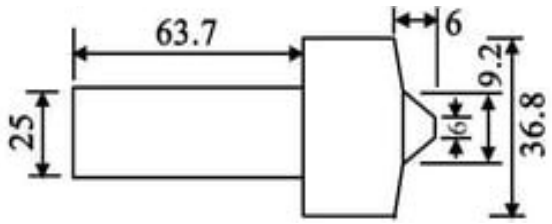

Figure 9: longitudinal micro-tensile

A steady-state three-dimensional heat conduction analysis was carried out considering the governing equation in equation 1 (Benlamnover *et al.*, 2021).

$$\frac{\partial}{\partial x}\left(k\frac{\partial T}{\partial x}\right)+\frac{\partial}{\partial y}\left(k\frac{\partial T}{\partial y}\right)+\frac{\partial}{\partial z}\left(k\frac{\partial T}{\partial z}\right)+Q=\rho C_p V\frac{\partial T}{\partial x} \quad (1)$$

Where v is the tool travel speed, T is the temperature variable, x, y, and z are spatial variables, and ρ, k, and C_p refer to the density, thermal conductivity, and specific heat of the workpiece materials, respectively.

The FSLW process was simulated, considering the Inconel 625 plate lapped onto the steel plate from the bottom until a depth of 0.5 mm. The tensile strength of a weld joint was measured by subjecting the standard

Corresponding author's email address: oginni.olarewaju@bouesti.edu.ng

specimens drawn from the test coupons to tensile tests as per ISO 4136:2001 using a universal testing machine. The hardness of different regions in the weld joint is measured by a Rockwell hardness test (ISO 9015-1 and 9015-2 standards) following the preparation of the preparation of a weld pad of size 80mm wide, 300mm long, and 3mm thick with run-on and run-off plates.

2.2 *Weld Geometry and Defect Test*

The bead width, such as welding current, welding speed, and gap distance, was determined by measuring the width of each welded sample with 0.01 mm least-count Vernier callipers for the mechanical qualities of the weld.

2.3 *Mechanical Property Testing*

For various mechanical tests, GMAW-welded experimental specimens were created from SS316 metals and machined using ASTM in order to determine the necessary dimensions for studying their properties**.**

2.4 *Tensile Strength*

A tensile test was conducted using a universal testing machine, a 600 servo-hydraulic with a piston speed of 8 mm/min and a maximum force of 600 KN.

2.5 *Hardness Testing*

The Rockwell hardness test was used because it was quick, inexpensive, and largely non-destructive, leaving a tiny indentation on the specimen. The hardness strength of the welded samples was examined using BROOKS Rockwell hardness testing equipment with a ball-shaped indenter at a force of 100 kg for a duration of 10 s.

2.6 *Design Expert*

The design matrix of three welding parameters via speed (S), wire feed rate (F), and voltage (V) at three levels was selected as the quality characteristic for the performance measure for 20 experimental runs, optimized, and tabulated.

2.7 *Response surface methodology (RSM)*

RSM was used to investigate the response of welding process parameters to the physical properties of INCONEL 625 and GL E36 steel based on design expert software. The welding speed, wire feed rate, and voltage were chosen as the independent variables, while the dependent variables (responses) were tensile strength and hardness values.

The quadratic response surface model built up all the linear terms, square terms, and linear by-linear interactions described in equation 2 (Tumer *et al.,* 2022).

$$Y=\beta_o + \varepsilon \sum_{i=1}^{k} \beta_i x_i + \sum_{i-1}^{k} \beta_{ij}\, x_i x_j + \sum_{i=1}^{k} \beta_{ii}\, x_i^2 + \varepsilon \quad (2)$$

Where Y is the predicted response; β_o is the overall mean,β_i is the linear effect of the input factors x_i; β_{ij} is the linear-by-linear interaction effect; $\beta_{ii}$is the quadratic effect of the input factor, $x_i\varepsilon$ is the random error term.

2.8 *Empirical Model*

The second-order polynomial model was used to describe the behaviour of the response to the inputs following the form presented in equation 3 (Wang *et al.*, 2020; Zhao *et al.*, 2021; Yang et al., 2022)

$$Y = X_0 + X_1(A) + X_2(B) + X_3(C) + X_{11}(A^2) + X_{22}(B^2) + X_{33}(C^2) + X_{12}(AB) + X_{13}(AC) + X_{23}(BC) \quad (3)$$

Where all X are constants and Y is the response.

Corresponding author's email address: oginni.olarewaju@bouesti.edu.ng

The developed empirical formulas in terms of the coded factors are given as equations 4 and 5 for tensile strength and hardness, respectively.

$$Y_1 = \{435.34 - 37.82A + 1.76B + 12.18C - 0.3750AB + 1.87AC + 0.1250BC - 2.62A^2 + 5.69B^2 + 5.51C^2\} \quad (4)$$

$$Y_2 = \{83.00 - 7.12A + 0.3661B + 2.35C - 0.1250AB + 0.3750AC - 0.1250BC - 0.6781A^2 + 1.09B^2 + 0.9129C^2\} \quad (5)$$

Y_1 is the tensile strength response, Y_2 is the hardness response, and A, B, and C represent the welding speed, wire feed rate, and voltage, respectively.

3. Results and Discussion

The results of the liquid penetrant and visual defect testing on the specimens were visually inspected and showed a few welding faults, such as a bit of undercut at the end, excessive reinforcement height, lack of fusion, porosity, root crack, and lack of penetration in some of the welded samples. There was a lack of fusion in one sample (20) due to minimum current input, arc length, electrode angle, electrode manipulation, and improper welding parameter settings, which contributed to the fusion failure. There was a porosity defect observed in a sample (14). This defect was created by air entrapped in the shielding gas, which resulted in dispersed porosity and gross surface pore breaking. An undercut defect was observed in samples 2 and 10. At the weld, undercut discontinuities formed a mechanical notch interface. Apart from the aforementioned, others were defect-free samples (1-20) used for the tensile strength and hardness tests in consonance with Mou *et al.* (2021) study.

Table 3 displays the tensile strength and hardness values of the welded samples based on the 20 experimental runs used for this study. The tensile strength and hardness values gotten from the experiment range between 380 and 500 MPa and 72 and 95 HRB, respectively. The large variance shows that process factors have an impact on the mechanical behavior of welded samples. The impact of welding input parameters such as welding speed, welding feed rate, and voltage is significant to the mechanical property responses. For instance, welding input parameters in the experimental run 7 with welding speed 52, welding feed rate 5.6, and voltage of 26 produced the highest value of tensile strength and hardness, i.e., 500 MPa and 95 HB, whereas the experimental run 10 with welding speed 68, welding feed rate of 5.1, and voltage of 24 v had the least tensile strength and hardness, i.e., 380 MPa and 72 HB. Increasing the welding feed rate from 5.1 to 5.6 increases the tensile strength from 380 to 500 MPa and the hardness value from 72 to 95 HB. There were 3 runs with the same input welding parameters given by the design expert, as seen in experimental runs 4, 16, and 17, with the same values of 58, 5.1, and 24 for welding speed, welding feed rate, and voltage, respectively, as shown in Table 3. There was no significant difference in their response values for both tensile strength and hardness. However, when the welding feed rate and voltage have the same values but different welding speeds, as seen in experimental runs 1, 4, 5, 8, and 17, there was significant variation in tensile strength and hardness. This is proof that the welding speed input parameter is the most significant factor that influences the tensile strength and hardness responses as contained in Satputaley *et al*., (2021) and Patel *et al*., (2020) works.

Corresponding author's email address: oginni.olarewaju@bouesti.edu.ng

Table 3: Experimental responses of tensile strength and hardness at different levels

S/N	Original Value			Responses	
	Welding, S(m/s)	Welding Feed Rate(m/min)	Voltage(v)	TS (MPa)	Hardness (HRD)
1	52	5.1	24	476	90
2	64	5.6	22	385	73
3	64	4.7	26	482	92
4	58	5.1	24	388	74
5	64	5.1	24	495	94
6	64	5.6	26	410	78
7	52	5.6	26	500	95
8	58	5.6	24	415	79
9	50	4.7	24	476	90
10	68	5.1	24	380	72
11	58	4.4	26	450	86
12	58	5.9	24	453	86
13	58	5.1	21	428	81
14	52	4.7	27	474	90
15	58	5.1	22	435	83
16	58	5.1	24	435	83
17	58	5.1	24	436	83
18	64	4.7	22	436	83
19	64	4.7	22	435	83
20	52	5.6	22	435	83

In reliability Table 4, the factors are considered significant when the adequacy of this model is analysed using ANOVA (and $p \leq 0.05$) and insignificant if otherwise. Accordingly, the developed models are significant. Welding speed (A) and voltage (C) are more significant than welding feed rate.

Corresponding author's email address: oginni.olarewaju@bouesti.edu.ng

Table 4: Determination of model significance using ANOVA

Source	Tensile Strength		Hardness	
	F Value	p- value	F Value	p-value
Model	29.18	< 0.0001	29.42	< 0.0001
A-Welding Speed	223.53	< 0.0001	211.37	< 0.0001
B-Welding feed rate	0.4911	0.4994	0.5585	0.4721
C- Voltage	23.51	0.0007	23.07	0.0007
AB	0.013	0.9113	0.0381	0.8491
AC	0.3262	0.5805	0.3432	0.5710
BC	0.0014	0.9704	0.0381	0.8491
A^2	1.05	0.3096	2.02	0.1855
B^2	5.41	0.0423	5.22	0.0454
C^2	5.08	0.0478	3.66	0.0846

*Note that the p-value of less than 0.0500 is an indication of model term significance.

Figure 10 (a-c) shows the effect of the input factors on the first response tensile strength. The three plots clearly show the level of significance of the selected welding speed and voltage on the tensile strength. It was discovered in Figure 10a that the welding speed has a better influence on hardness than the welding feed rate because the hardness deviates more from the welding speed than the welding feed rate. Figure 10b depicts a better response of welding speed compared to the voltage, and Figure 10c shows that hardness has a better response to the voltage compared to the welding feed rate. The hardness responses obtained from all the input parameters follow the same trend when compared to the tensile strength response, while the welding feed rate showed the least significant effect on hardness.

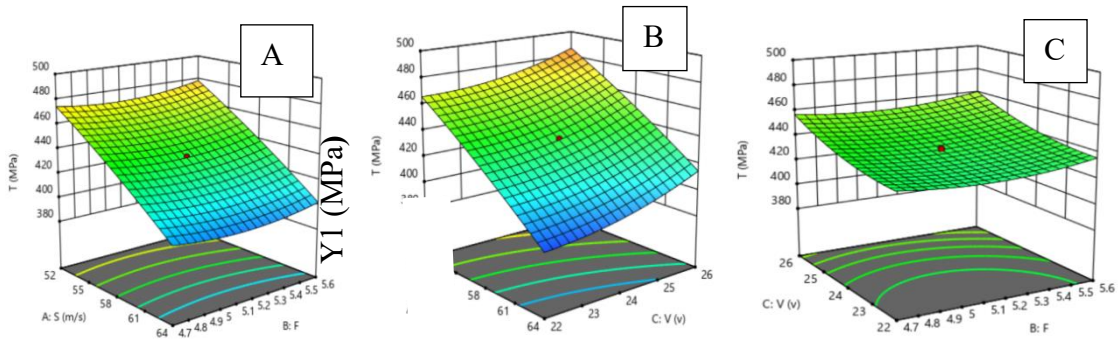

Figure 10: 3D plots of tensile strength against (a) welding speed and welding feed rate (b) welding speed and voltage (c) voltage and welding feed rate

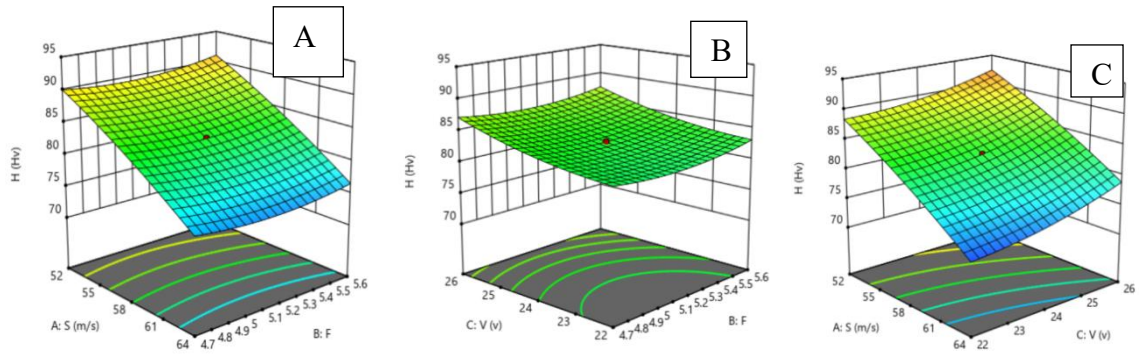

Figure 11: 3D plots of hardness against (a) welding speed and welding feed rate (b) welding speed and voltage (c) voltage and number of passes

As indicated in Table 5, R^2 of 0.9633 and 0.9611 for both tensile strength and hardness and adequate precisions of 19.7960 and 19.284 for both tensile strength and hardness imply a good fit. Other variables also support the fact that the model is adequate and reliable, and can be used to navigate the design space.

Table 5: Second Order Model Fitting Results in the Form of ANOVA

Model Summary Characteristics	Tensile strength	Hardness
Standard Deviation	9.29	1.81
Mean	441.20	83.9
R^2	0.9633	0.9611
Adjusted R^2	0.9303	0.9260
Predicted R^2	0.7216	0.7040
Adequate Precision	19.7960	19.284

The value of the output factors at optimum for the given input parameters with a maximum desirability of 1 and for the combined results that are derived from the software. The tensile strength and hardness generated from the empirical model developed have been validated with the use of experimental results and were compared as presented in Table 6.Three confirmation experiments were conducted at the optimum process welding parameters of 53 welding speed, 5 welding feed rate, and 23 voltage that were predicted by the software. The details of the experimental designs were reported in Figure 12 (Zhang *et al*., 2020).

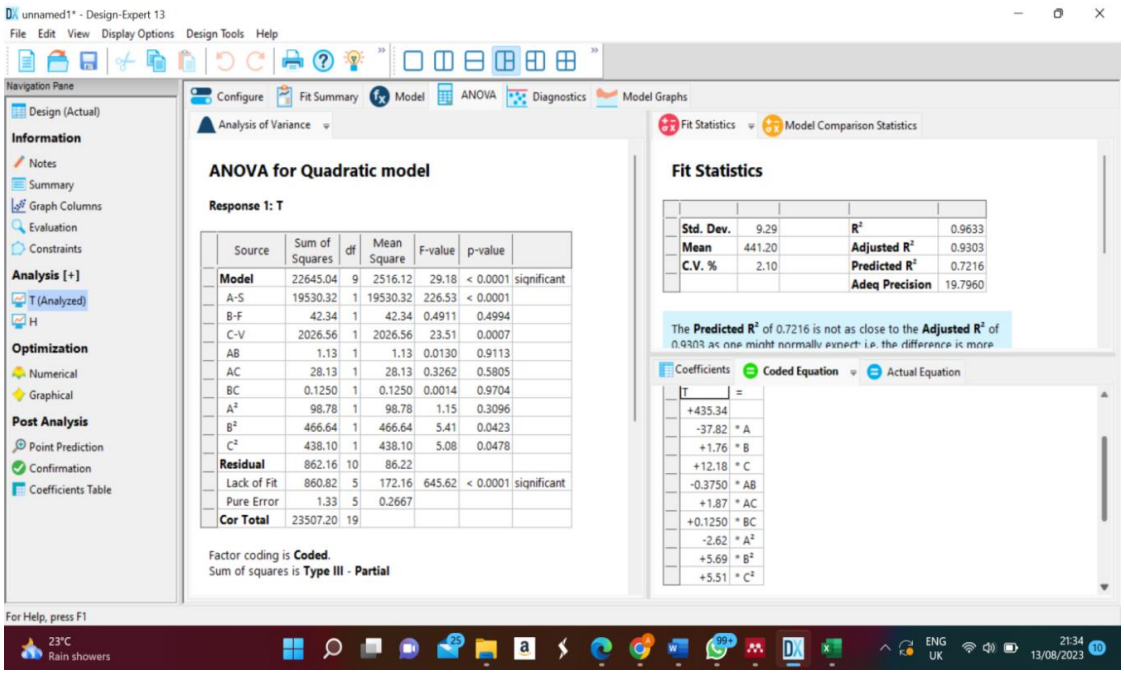

Figure 12: Tensile strength Response ANOVA

Corresponding author's email address: oginni.olarewaju@bouesti.edu.ng

Table 6: Predicted and experimental results for tensile strength and Hardness

Standard	Input			Tensile S		Hardness	
	WS	WFR	Voltage	Actual	Predicted	Actual	Predicted
1	52	5.1	24	435.00	435.34	83.00	83.00
2	64	5.6	22	415.00	421.67	79.00	80.04
3	64	4.7	26	476.00	491.53	90.00	93.06
4	58	5.1	24	453.00	454.39	86.33	86.69
5	64	5.1	24	453.00	435.34	83.00	83.00
6	64	5.6	26	428.00	430.45	81.00	81.62
7	52	5.6	26	495.00	489.79	94.00	93.05
8	58	5.6	24	482.00	473.44	92.00	90.08
9	48	4.7	24	390.00	364.33	72.00	69.10
10	68	5.1	24	435.00	435.34	83.00	83.00
11	58	4.4	26	388.00	393.31	74.00	74.84
12	58	5.9	24	476.00	469.42	90.00	88.85
13	58	5.1	21	410.00	418.65	78.00	79.81
14	52	4.7	27	385.00	390.79	73.00	74.10
15	58	5.1	22	435.00	435.34	83.00	83.00
16	58	5.1	24	474.00	471.42	90.00	89.54
17	58	5.1	24	500.00	494.31	95.00	93.79
18	64	4.7	22	450.00	448.47	86.00	85.46
19	64	4.7	22	436.00	435.34	83.00	83.00
20	52	5.6	22	436.00	435.34	83.00	83.00

Note: WS = Welding speed and WFR = welding feed rate

4. Conclusion

The right selection of welding process and responses of tensile strength and hardness by optimizing the welding parameters during the welding of INCONEL 625 and GL E360 steels in the operation have been investigated and established. The parameters have a significant impact in relation to the input independent variables (such as welding speed, welding feed rate, and voltage) and the response variables (such as tensile strength and hardness). Various defects in welding technologies have been eliminated by using the correct combination of welding process parameters, technical know-how, response surface methodology, and optimization tools. The tensile strength falls between 380 and 500 MPa, and the hardness is between 72 and 95 HRD. The variation in the responses shows that the combination of the selection of welding process parameters has a significant impact on the machining operations. The impact of a welding speed of 52, a welding feed rate of 5.6, and a

Corresponding author's email address: oginni.olarewaju@bouesti.edu.ng

voltage of 26 (run 7) proved to be the most noticeable effect, with the highest tensile strength of 500 MPa and a hardness of 95 HRD.The welding process parameters have the highest significant factor in tensile strength, followed by the voltage. The welding feed rate parameter is the least significant in both tensile strength and harness responses.

The value of the output factors at optimum for the welding parameters at maximum desirability of 1 and for the combined results that are derived from the software was obtained. The surface response methodology optimizes the best welding process parameters for quality weld joints and products, and enhances productivity. This study provides relevant data for developing, investigating, and evaluating the model and performance evaluation of the welding problems, specifically the tensile strength and hardness of INCONEL 625 and GL E60 steels.

References

Alagarsamy, SV. and Kumar, R. 2019. Parametric optimization for gas metal arc welding process of SS316L and AISI D2 steels using Grey-Taguchi method. Journal of Materials Science Research and Reviews, 4(3): 402-411.

Arunkumar, SP., Prabha, C., Saminathan, D., Rajasekaran, KJA., Viswanath, M., Ivan, C., Kevin, P. and Kumar, PM. 2022. Taguchi optimization of metal inert gas (MIG) welding parameters to withstand high impact load for dissimilar weld joints. Materials Today, 56(2): 1411-1417.

Assefa, A., Teferi, A., Gulam, MS., Alamri, S., Edacherian, AJ., Moera, G., Pandey, V. and Hossain, N. 2022. Experimental investigation and parametric optimization of the tungsten inert gas welding process parameters of dissimilar metals. Materials, 15(13): 4426-4435.

Benlamnouar, MF., Saadi, T., Bensaid, N., Gousmine, M., Touggui, Y. and Temmar, M. 2021. Modelling and optimization of dissimilar welding between 304L and HSLA-X70 using response surface methodology. Journal of Advanced Manufacturing Technology, 105(5): 24-26.

Beygi, R., Galvão, I., Akhavan-Safar, A., Pouraliakbar, H., Fallah, V. and da Silva, LF. 2023. Effect of alloying elements on intermetallic formation during friction stir welding of dissimilar metals: A critical review on aluminum/steel.Metals, 13(4): 768-773.

Bossle, EP., Vicharapu, B., Lemos, GV., Lessa, CR., Bergmann, L., Santos, JF. and Amitava, D. 2023. Friction stir lap welding of inconel 625 and a high strength steel. Metals, 13(1): 146-157.

Buffa, G., Fratini, L., LaCommare, U., Römisch, D., Wiesenmayer, S., Wituschek, S. and Merklein, M. 2022. Joining by forming technologies: current solutions and future trends. International Journal of Material Forming, 15(3): 27-39.

Cooke, KO., Alhazaa, A. and Atieh, AM. 2019. Dissimilar welding and joining of magnesium alloys: Principles and application. The Wonder Element for Engineering/Biomedical Applications, 20(2): 94-110.

Dak, G. and Pandey, C. 2021. Experimental investigation on microstructure, mechanical properties, and residual stresses of dissimilar welded joint of martensitic P92 and AISI 304L austenitic stainless steel. International Journal of Pressure Vessels and Piping, 194: 104-112.

Devanathan, C., Babu, AS., Murugan, SS., Shankar, E. and Giri, R. 2022. Review of joining various materials by FSW process and applications. Welding and Technology, 33(2): 75-88.

Johnson, P. and Murugan, N. 2020. Microstructure and mechanical properties of friction stir welded AISI321 stainless steel. Journal of Materials Research and Technology, 9(3): 3967-3976.

Kannan, AR., Shanmugam, NS. and Vendan, SA. 2019. Effect of cold metal transfer process parameters on microstructural evolution and mechanical properties of AISI 316L tailor welded blanks. The International Journal of Advanced Manufacturing Technology, 103: 4265-4282.

Corresponding author's email address: oginni.olarewaju@bouesti.edu.ng

Khrais, S., Al H., Hadeel, A., Ahmad, A. and Darabseh, T. 2023. Impact of gas metal arc welding parameters on bead geometry and material distortion of AISI 316L. Journal of Manufacturing and Materials Processing, 7(4): 123-132.

Kumar, N., Pandey, C. and Kumar, P. (2023). Dissimilar welding of Inconel alloys with austenitic stainless-steel: A review. Journal of Pressure Vessel Technology, 145(1): 11-15.

Li, W., Xie, D., Li, D., Zhang, Y., Gao, Y. and Liaw, PK. 2021. Mechanical behavior of high-entropy alloys. Progress in Materials Science, 118(2): 100-117.

Luo, AA., Sachdev, AK. and Apelian, D. 2022. Alloy development and process innovations for light metals casting. Journal of Materials Processing Technology, 306(3): 117-124.

Madhavadas, V., Srivastava, D., Chadha, U., Raj, SA., Sultan, MH., Shahar, FS. and Shah, AU. 2022. A review on metal additive manufacturing for intricately shaped aerospace components. CIRP Journal of Manufacturing Science and Technology, 39(2):18-36.

Mou, G., Zheng, K., Shen, C., Xiang, H., Hua, X. and He, L. 2021. Microstructure investigation and fracture mechanism of TC4− 304L dissimilar joints fabricated by the cold metal transfer arc-brazing method. Journal of Materials Research and Technology, 15(5): 6758-6768.

Patel, GC., Manjunath, C., Ganesh, R., Paragoudar, MB., Gupta, K., Chate, G. R. and Gupta, K. 2020. Introduction to hard materials and machining methods: A comprehensive approach to experimentation, modeling and optimization. Journal of Materials and Technology, 36(3): 1-24.

Raju, TR. and Kumar, S. 2022. The weldability of AISI 1020 mild steel using autogenous tungsten inert gas (TIG) welding: an experimental study. Journal of Industrial Mechanics 7(3): 41-47.

Ramadan, N. and Boghdadi, A. 2020. Parametric optimization of TIG welding influence on tensile strength of dissimilar metals SS-304 and low carbon steel by using Taguchi approach. American Journal of Engineering Resources, 9(9): 7-14.

Ren, J., Xu, W., Yang, L., Wang, Z. and Li, Y. 2022. Study on vapor phase corrosion inhibitor for E36 ship steel in marine atmospheric environment: anti-corrosion methods. Materials, 69(4): 362-370.

Satputaley, SS., Waware, Y., Ksheersagar, K., Jichkar, Y. and Khonde, K. 2021. Experimental investigation on effect of TIG welding process on chromoly 4130 and aluminum 7075-T6. Materials Today, 41(2): 991-994.

Sivasubramani, R., Verma, A., Rithvik, G., Chadha, U. and Kumaran, SS. 2021. Influence on nonhomogeneous microstructure formation and its role on tensile and fatigue performance of duplex stainless steel by a solid-state welding process. Materials Today, 46(4): 7284-7296.

Stoll, A. and Benner, P. 2021. Machine learning for material characterization with an application for predicting mechanical properties. GAMM-Mitteilungen, 44(1): 20-26.

Tesfaye, FK. 2023. Parameter optimizations of GMAW process for dissimilar steel welding. The International Journal of Advanced Manufacturing Technology, 34(1): 1-8.

Tümer, M., Schneider, C. and Enzinger, N. 2022. Fusion welding of ultra-high strength structural steels: A review. Journal of Manufacturing Processes, 82(4): 203-229.

Wang, H., Liu, X. and Liu, L. 2020. Research on laser-TIG hybrid welding of 6061-T6 aluminum alloys joint and post heat treatment. Metals, 10(1): 130-139.

Wen, Q., Li, WY., Wang, WB., Wang, FF., Gao, YJ. and Patel, V. 2019. Experimental and numerical investigations of bonding interface behavior in stationary shoulder friction stir lap welding. Journal of Materials Science & Technology, 35(1): 192-200.

Corresponding author's email address: oginni.olarewaju@bouesti.edu.ng

Yang, J., Oliveira, JP., Li, Y., Tan, C., Gao, C., Zhao, Y. and Yu, Z. 2022. Laser techniques for dissimilar joining of aluminum alloys to steels: a critical review. Journal of Materials Processing Technology, 301(3): 117-123.

Zhang, YM., Yang, Y., Zhang, W. and NA, S. 2020. Advanced welding manufacturing: a brief analysis and review of challenges and solutions. Journal of Manufacturing Science and Engineering, 142(11): 96-108.

Zhao, Y., Koizumi, Y., Aoyagi, K., Yamanaka, K. and Chiba, A. 2021. Thermal properties of powder beds in energy absorption and heat transfer during additive manufacturing with electron beam. Powder Technology, 38(1): 44-54.

Corresponding author's email address: oginni.olarewaju@bouesti.edu.ng